J.Natn.Sci.Foundation Sri Lanka 2026 54 (1): 17 - 30
DOI: http://dx.doi.org/10.4038/jnsfsr.v54i1.12522

RESEARCH ARTICLE

Statistics

Versatility in control theory and real-world applications

R Jabeen[1*], FM Alghamdi[2], HM Aljohani[3] and A Zaka[4]
[1] *Department of Statistics, COMSATS University Islamabad, Lahore Campus, Lahore, Pakistan.*
[2] *Department of Mathematical Sciences, College of Science, Princess Nourah bint Abdulrahman University, Riyadh 11671, Saudi Arabia.*
[3] *Department of Mathematics and Statistics, College of Science, Taif University, Taif 21944, Saudi Arabia.*
[4] *Department of Statistics, Government Graduate College of Science, Wahdat Road, Lahore, Pakistan.*

Submitted: 17 March 2025; Revised: 28 January 2026; Accepted: 18 February 2026

Abstract: The inspiration of this manuscript is reflected power function (RPF) and size biased distributions. We present a size-biased reflected power function (SBRPF) distribution using highly flexible reflected power function distribution. The resulting distribution is also flexible enough to fit all types of data either J shaped, reverse J shaped, positive skewed and negative skewed. We also drive various important properties of the suggested model. We show the comprehensive analysis of the proposed model detailing the asymptotic behavior of the function. We use diverse methods of estimation such as modified maximum likelihood method (MMLM) , maximum likelihood method (MLE) , percentile estimator (PE). The numerical analysis shows that the SBRF distribution remains consistent while mean square error (MSE) does not decrease as sample size increases. The real life data sets demonstrate that SBRPF distribution is a better choice to be compared with other models exist in the literature. We also reported the use of two control charts Exponential weighted moving averages (EWMA) and Extended Exponentially weighted moving averages (EEWMA) for the shape parameter of the proposed model. From both Simulation studies and real life application, we observe that EEWMA is a more effective control chart for detecting early change during a process for SBRPF distribution.

Keywords: Failure rate components, power function distribution, reflected distribution, size-biased distribution.

INTRODUCTION

In engineering and related fields, researchers typically aim to assess the reliability of a module over a specified period under defined conditions. This need urges the new researchers to employ some new flexible distributions to model the lifetime data of different engineering processes. Probability distributions are used to draw meaningful inferences from real life problems and analyze the variations in the data. The probability distributions basically represent the variability in the random variables. Due to the continuous evolve in technology, the complexity of data increases and the existing distribution falls short of capturing all trends in data. Keeping in view these circumstances, efforts are made to produce new distributions, and some modifications are proposed to the existing distributions. These efforts include generalization, compounding and mixing the already existing distributions.

In this research, we incorporate reflected power and size-biased distributions to develop a unique distribution. Basically, reflected power function (RPF) distribution [1] is given as a modification of power function (PF) distribution. This model is famous for its flexibility in modeling lifetime data and good for fitting certain failure data sets. As claimed in [2], the PF distribution is interconnected to the Pareto distribution. The authors of [3] explore the PF distribution as a preferable choice over others for assessing the durability of semiconductor devices and products.

The one particular case for weighted distribution is named as the size-biased distribution. It was first

* Corresponding author (drriffatjabeen@cuilahore.edu.pk; https://orcid.org/0000-0003-1461-0611)

introduced by [4] in the context of bias modeling and later expanded into a unified theory by [5]. In practice, this type of distribution often arises when sample observations are recorded with unequal probabilities, such as in probability proportionate to size (PPS) sampling designs.

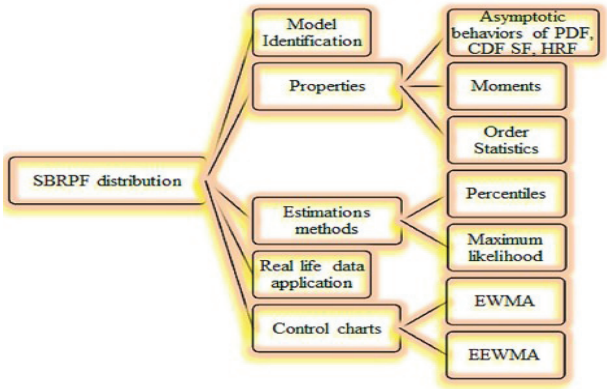

The size-biased distribution can be obtained using

$$f_s(x) = \frac{x^{\alpha} f(x)}{E[x^{\alpha}]},$$

where $f(x)$ is the baseline distribution, $w(x)$ is weight function. It is compulsory that the term $E[x^{\alpha}]$ exist.

A particularly interesting case occurs as the weight function becomes $w(x) =$ which is known as sized-biased distribution. For more details, please refer to [6]–[8].

The application of weighted distributions is discussed details by [9]. Subsequently, [10] analyzed HPS diameter increment data and applied weighted distributions. More recently, [11] utilized weight distributions to model a stochastic population with predictive effects, employing a stochastic differential equation to compute the gamma distribution as a weight for the stationary probability density function (PDF).

Taillie et al. [12] applied weighted distributions to sample fish stock populations. Also, Gove and Patil [13] used the same theory for the quadratic relationship between diameter and basal area. In both above literature, the said distributions served as straightforward model for the observed data.

The aim of this research is to apply size-biased distribution theory to real-world data. For this we propose the size-biased reflected power function (SBRPF) distribution as a modification to power function distribution (PFD) introduced in [14].

The SBRPF distribution is highly versatile due to its straightforward formulation, making it applicable in reliability engineering, biosciences, and forestry. The parameters of the proposed distribution will be estimated using MLE, MMLM, and MPE. Additionally, we will demonstrate the practical application of the SBRPF distribution.

The weighted distributions, introduced by [4] and further developed by [6], includes size-biased and area-biased distributions as special cases. These distributions naturally arise in practice when sample observations are recorded with unequal probabilities Additionally, the transmuted weighted exponential [15] and other weighted distributions are given by [16].

Control charts have become crucial tools for monitoring product quality across various sectors, particularly in agriculture and industry. It was [17] who introduced. The exponentially weighted moving average (EWMA). Then [18] provided modified EWMA (MEWMA) control chart for monitoring the scale parameter of Weibull distribution. The EWMA was modified by [19] and named as exponentially EWMA (EEWMA) control chart.

A new EWMA control chart, based on the log transformation of sample variance, was discussed in [20]. This new chart was compared with several conventional charts. Additionally, [21]-[26] explored new additional monitoring charts

Model identification

The power function (PF) distribution is defined as

$$f_{PF}(y) = \frac{\gamma y^{\gamma-1}}{\beta^{\gamma}}, \qquad 0 < y < \beta. \qquad ...(1)$$

where γ and β is shape and scale parameter.

The RPF distribution is defined as

$$f_{RPF}(x) = \frac{\gamma(\theta-x)^{\gamma-1}}{\beta^{\gamma}}, \quad \theta-\beta < x < \theta. \qquad ...(2)$$

where γ and β is shape and scale parameter. Also θ is reflecting parameter.

The PDF and cumulative distribution function (CDF) of the SBRPF distribution is given as

$$f_{SBRPF}(x) = \frac{x\gamma(\theta-x)^{\gamma-1}(\gamma+1)}{\beta^{\gamma}\{\theta(\gamma+1)-\beta\gamma\}}, \qquad \theta-\beta < x < \theta. \quad ...(3)$$

$$F_{SBRPF}(x) = \frac{(\theta-x)^{\gamma}(x\gamma+\theta)+\beta^{\gamma}\{\beta\gamma-\theta(\gamma+1)\}}{\beta^{\gamma}\{\beta\gamma-\theta(\gamma+1)\}}. \quad ...(4)$$

The survival function (SF), hazard rate function (HRF) and quantile function (QF) for SBRPF distribution are given by:

$$S_{SBRPF}(x) = 1 - \frac{(\theta-x)^{\gamma}(x\gamma+\theta)+\beta^{\gamma}\{\beta\gamma-\theta(\gamma+1)\}}{\beta^{\gamma}\{\beta\gamma-\theta(\gamma+1)\}}. \quad ...(5)$$

$$h_{SBRPF}(x) = \frac{x\gamma(\gamma+1)}{(\theta-x)(x\gamma+\theta)} \quad ...(6)$$

and

$$x_p = [\theta^2 - \beta\{\beta - 2\theta\}(p_i - 1)]^{1/2}. \quad ...(7)$$

Note that x_p can be used to generate the SBRPF random values.

Special cases

We reported two special cases of our proposed distribution which are given below

1. Multiplying SBRPF distribution by the quantity $\frac{\theta(\gamma+1)-\beta\gamma}{x(\gamma+1)}$, gives the density function of the RPF distribution.
2. Multiplying SBRPF distribution by $\frac{\theta(\gamma+1)-\beta\gamma}{x(\gamma+1)}$ and then by putting $x = \theta - y$, we obtain the PF distribution.

Two special cases are presented in Figure 1, which provides the loop of both cases.

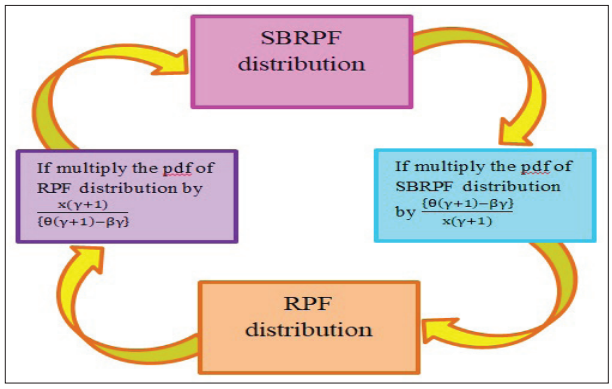

Figure 1: Probability distributions loop plot.

Figure 1 shows probability distributions loop plot which shows that we can get SBRPF from RPF distribution and similarly we get RPF distribution from SBRPF model as a special case by multiplying with $\frac{(\theta(\gamma+1)-\beta\gamma)}{x(\gamma+1)}$.

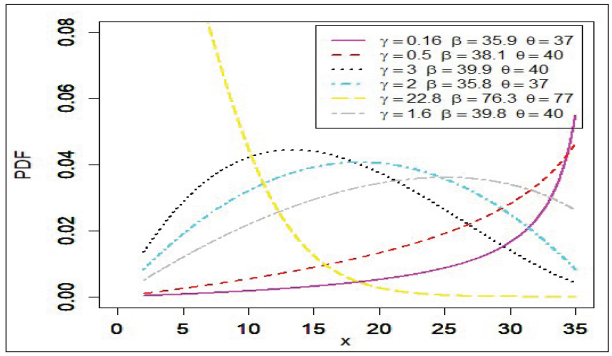

Figure 2: Probability density function of the SBRPF distribution.

Figures 2 and 3 present the plots of the PDF of the SBRPF distribution. The PDF plots demonstrate that this proposed distribution can effectively fit a wide variety of data types, including positively skewed, negatively skewed, J-shaped, reversed-J-shaped, and symmetric data.

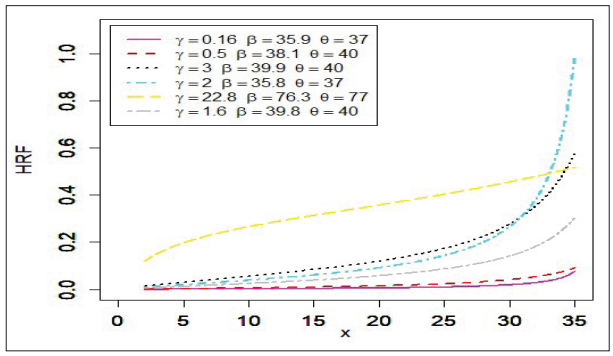

Figure 3: Plots for the HRF of the SBRPF distribution.

Figure 3 presents the plots of the HRF of the SBRPF distribution. The HRF plot demonstrates that this proposed distribution can effectively fit a wide variety of data types, including positively skewed, negatively skewed, J-shaped, reversed-J-shaped, and symmetric data.

Properties of SBRPF distribution

In this section various properties of the SBRPF distribution are discussed.

Limiting behaviors of SBRPF distribution

The limiting behaviors of the SBRPF distribution, for $x \to 0$ and $x \to \infty$, are given by

1. $\lim_{x\to 0} f_{SBRPF}(\mathrm{x}) = \lim_{x\to 0} \frac{\mathrm{x}\gamma(\theta-\mathrm{x})^{\gamma-1}(\gamma+1)}{\beta^{\gamma}\{\theta(\gamma+1)-\beta\gamma\}}.$

2. $\lim_{x\to \infty} f_{SBRPF}(\mathrm{x}) = \lim_{x\to \infty} \frac{\mathrm{x}\gamma(\theta-\mathrm{x})^{\gamma-1}(\gamma+1)}{\beta^{\gamma}\{\theta(\gamma+1)-\beta\gamma\}} = \infty.$

3. $\lim_{x\to 0} F_{SBRPF}(\mathrm{x}) = \lim_{x\to 0} \frac{(\theta-\mathrm{x})^{\gamma}(\mathrm{x}\gamma+\theta)+\beta^{\gamma}\{\beta\gamma-\theta(\gamma+1)\}}{\beta^{\gamma}\{\beta\gamma-\theta(\gamma+1)\}} = 0,$ for $\gamma = 1, \beta = 0, \theta = 0.$

4. $\lim_{x\to \infty} F_{SBRPF}(\mathrm{x}) = \lim_{x\to \infty} \frac{(\theta-\mathrm{x})^{\gamma}(\mathrm{x}\gamma+\theta)+\beta^{\gamma}\{\beta\gamma-\theta(\gamma+1)\}}{\beta^{\gamma}\{\beta\gamma-\theta(\gamma+1)\}} = 1,$ for $\gamma = 0, \beta = 1, \theta = 0.$

5. $\lim_{x\to 0} S_{SBRPF}(\mathrm{x}) = \lim_{x\to 0} 1 - \frac{(\theta-\mathrm{x})^{\gamma}(\mathrm{x}\gamma+\theta)+\beta^{\gamma}\{\beta\gamma-\theta(\gamma+1)\}}{\beta^{\gamma}\{\beta\gamma-\theta(\gamma+1)\}} = 1,$ for $\gamma = 1, \beta = 0, \theta = 0.$

6. $\lim_{x\to \infty} S_{SBRPF}(\mathrm{x}) = \lim_{x\to \infty} 1 - \frac{(\theta-\mathrm{x})^{\gamma}(\mathrm{x}\gamma+\theta)+\beta^{\gamma}\{\beta\gamma-\theta(\gamma+1)\}}{\beta^{\gamma}\{\beta\gamma-\theta(\gamma+1)\}} = 0,$ for $\gamma = 0, \beta = 1, \theta = 0.$

7. $\lim_{x\to 0} h_{SBRPF}(\mathrm{x}) = \lim_{x\to 0} \frac{\mathrm{x}\gamma(\gamma+1)}{(\theta-\mathrm{x})(\mathrm{x}\gamma+\theta)} = 0.$

8. $\lim_{x\to \infty} h_{SBRPF}(\mathrm{x}) = \lim_{x\to \infty} \frac{\mathrm{x}\gamma(\gamma+1)}{(\theta-\mathrm{x})(\mathrm{x}\gamma+\theta)} = 0,$ for $\gamma = 0, \theta = 0.$

Moments

The r^{th} moment about zero of SBRPF is below as

$$\mu_r = \frac{v(v+1)\theta^{r+v+1}}{\beta^{v}(\theta(v+1)-v\beta)} \sum_{j=0}^{\infty} \frac{(-1)^j(\Gamma v)\left(1-\left(\frac{\theta-\beta}{\theta}\right)^{(r+j+2)}\right)}{(\Gamma v-j)j!(r+j+2)} \quad \ldots(8)$$

The moment generating function defines the characteristics of a random variable.

$$M_o(t) = \frac{v(v+1)}{\beta^{v}\{\theta(v+1)-\beta v\}} \sum_{r=0}^{\infty} \frac{t^r}{r!} \theta^{v+r+1} \sum_{j=0}^{\infty} \frac{(-1)^j \Gamma v}{(\Gamma v-j)j!} \left\{ \frac{1-\left(\frac{\theta-\beta}{\theta}\right)^{r+j+2}}{r+j+2} \right\} \quad \ldots(9)$$

Order statistics

The density function of j^{th}, largest and smallest order statistics of the SBRPF distribution is obtained as

$$g_{(j)}(x) = \frac{n!}{(j-1)!\,(n-j)!}\left[\frac{x\gamma(\theta-x)^{\gamma-1}(\gamma+1)}{\beta^{\gamma}\{\theta(\gamma+1)-\beta\gamma\}}\right]\left[\frac{(\theta-x)^{\gamma}(x\gamma+\theta)+\beta^{\gamma}\{\beta\gamma-\theta(\gamma+1)\}}{\beta^{\gamma}\{\beta\gamma-\theta(\gamma+1)\}}\right]^{j-1}$$
$$\left[1-\frac{(\theta-x)^{\gamma}(x\gamma+\theta)+\beta^{\gamma}\{\beta\gamma-\theta(\gamma+1)\}}{\beta^{\gamma}\{\beta\gamma-\theta(\gamma+1)\}}\right]^{n-j}. \quad ...(10)$$

$$g_{(n)}(x) = n\left[\frac{x\gamma(\theta-x)^{\gamma-1}(\gamma+1)}{\beta^{\gamma}\{\theta(\gamma+1)-\beta\gamma\}}\right]\left[\frac{(\theta-x)^{\gamma}(x\gamma+\theta)+\beta^{\gamma}\{\beta\gamma-\theta(\gamma+1)\}}{\beta^{\gamma}\{\beta\gamma-\theta(\gamma+1)\}}\right]^{n-1}. \quad ...(11)$$

$$g_{(1)}(x) = n\left[\frac{x\gamma(\theta-x)^{\gamma-1}(\gamma+1)}{\beta^{\gamma}\{\theta(\gamma+1)-\beta\gamma\}}\right]\left[1-\frac{(\theta-x)^{\gamma}(x\gamma+\theta)+\beta^{\gamma}\{\beta\gamma-\theta(\gamma+1)\}}{\beta^{\gamma}\{\beta\gamma-\theta(\gamma+1)\}}\right]^{n-1}. \quad ...(12)$$

Parameters estimation of the SBRPF

The parameters of SBRPF are estimated with two PE and MLE. The results are obtained using the R programming language. These estimation methods have also been employed in studies [30]-[34].

Percentile estimators

The PE was given by [35]-[36]. Let $p_i = i/n + 1$ be an unbiased estimator of $F_{SBRPF}(x_{(i)};\gamma,\beta,\theta) = \frac{(\theta-x)^{\gamma}(x\gamma+\theta)+\beta^{\gamma}\{\beta\gamma-\theta(\gamma+1)\}}{\beta^{\gamma}\{\beta\gamma-\theta(\gamma+1)\}}$, the PE of the parameters from SBRPF obtained as after minimizing the following function

$$P(\gamma,\beta,\theta) = \sum_{i=1}^{n}\left[x_{(i)} - [\theta^2 - \beta\{\beta-2\theta\}(p-1)]^{1/2}\right]^2, \quad ...(13)$$

with respect to γ, β and θ.

Maximum likelihood estimators

SBRPF model's log-likelihood function reduces to

$$\ell(x) = \sum_{i=1}^{n}\log(x_i) + n\log(\gamma) + (\gamma-1)\sum_{i=1}^{n}(\theta-x_i)$$
$$+ n\log(\gamma+1) - \log(\beta)^{n\gamma} - n\log(\theta) - n\log(\gamma+1)$$
$$+ n(\gamma+1)\log(\beta) + n\log(\gamma). \quad ...(14)$$

We can get MLE of the parameters by maximizing the log-likelihood function.

Numerical analysis

We generated random numbers using SBRPF distribution. We use different combinations of parameters to numerically compare PE and MLE. For three sample sizes: n = 150, 250 and 400 results are generated. We repeated the procedure for N = 2000, during which the SBRPF parameters are estimated for each parameter combination and sample using both the PCE and MLE. The average values (Avg) of the estimates and mean square errors (MSE) are reported for all samples.

Method validation

From Table 1, it is clear that all estimation methods exhibit the consistency; specifically, for all combinations of parameters, the MSE decreases as we increase the n.

Real-life applications

The actual dataset consists of failure times for 20 components [37] is considered to compare the performance of proposed distributions. We compared the proposed model with the reflected power function (RPF) [1] and the size-biased Mukherjee-Islam (SBMI) distribution [38]. The Kolmogorov-Smirnov (KS) test and its p-value, as well as the Hannan-Quinn information

criterion (HQIC), Akaike information criterion (AIC), consistent AIC (CAIC), negative log-likelihood function (-log($\hat{\theta}$)) and Bayesian information criterion (BIC),were used to make the comparison.

Table 1: Average and MSE of the SBRPF parameters for various sample sizes.

Methods	n	Parameters			Avg of estimates			MSE		
		γ	β	θ	Avg$(\hat{\gamma})$	Avg$(\hat{\beta})$	Avg$(\hat{\theta})$	MSE$(\hat{\gamma})$	MSE$(\hat{\beta})$	MSE$(\hat{\theta})$
PCE	150	1	2.1	5	7.00012	2.09933	4.99971	36.00144	0.00301	0.00136
	250				1.00952	2.09973	5.00122	0.00009	0.00180	0.00088
	400				1.00021	2.10086	4.99962	0.00000	0.00112	0.00055
	150	1	1.9	4	5.43512	1.90188	4.00093	19.67029	0.00264	0.00113
	250				1.00323	1.89998	3.99930	0.00001	0.00148	0.00068
	400				1.00008	1.90164	4.00026	0.00000	0.00091	0.00042
	150	1	1.5	2	1.74984	1.50452	1.99892	0.56226	0.00249	0.00056
	250				1.00027	1.50495	1.99942	0.00000	0.00146	0.00034
	400				1.00001	1.50107	1.99941	0.00000	0.00082	0.00022
MLE	150	1	2.1	5	18.95848	3.72082	4.99939	322.50761	2.62707	0.00060
	250				2.46269	2.87735	4.99939	2.13946	0.60427	0.00016
	400				1.00376	2.10808	4.99930	0.00001	0.00007	0.00004
	150	1	1.9	4	15.08033	3.08278	3.99940	198.25580	1.39896	0.00037
	250				2.51481	2.69164	3.99934	2.29466	0.62670	0.00011
	400				1.00339	1.90719	3.99926	0.00001	0.00005	0.00003
	150	1	1.5	2	3.87385	1.93599	1.99934	8.25931	0.19009	0.00013
	250				1.00378	1.50711	1.99928	0.00001	0.00005	0.00003
	400				1.00116	1.50235	1.99935	0.00000	0.00001	0.00001

Table 2: Descriptive statistics summary of real data.

Minimum	1st Quartile	Median	Mean	3rd Quartile	Maximum
0.072	4.471	8.662	8.429	11.648	19.809

Table 2 presents a concise summary of the statistical data. It provides us with minimum and maximum values in the data. Also provide us mean, median and quartile values of the data.

Table 3: The MLEs, and goodness-of-fit measures for failure time of 20 components.

Model	MLEs	KS	p-value	AIC	BIC	CAIC	HQIC	$-\log(\hat{\theta})$
SBRPF	2.4764 19.7978 20.4586	0.14846	0.716	135.0122	137.9994	136.5122	135.5953	64.5061
RPF	3.4010 19.7904 19.9185	0.45654	0.0002	154.0047	156.9919	155.5047	154.5879	74.00236
SBMI	8.958771 19.9749	0.87201	0.0000	498.8489	500.8404	499.5548	499.2376	247.4244

Table 3 reports the MLE and all other measures for comparison among the distributions. The data in this table indicates that the SBRPF is superior for the studied data compared to the competing models.

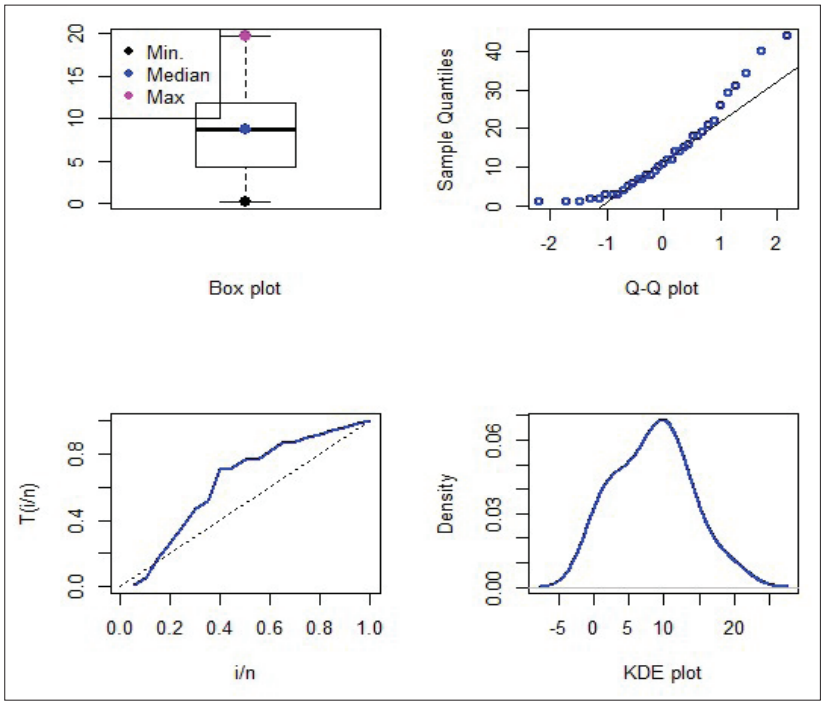

Figure 6: Plots of the real dataset.

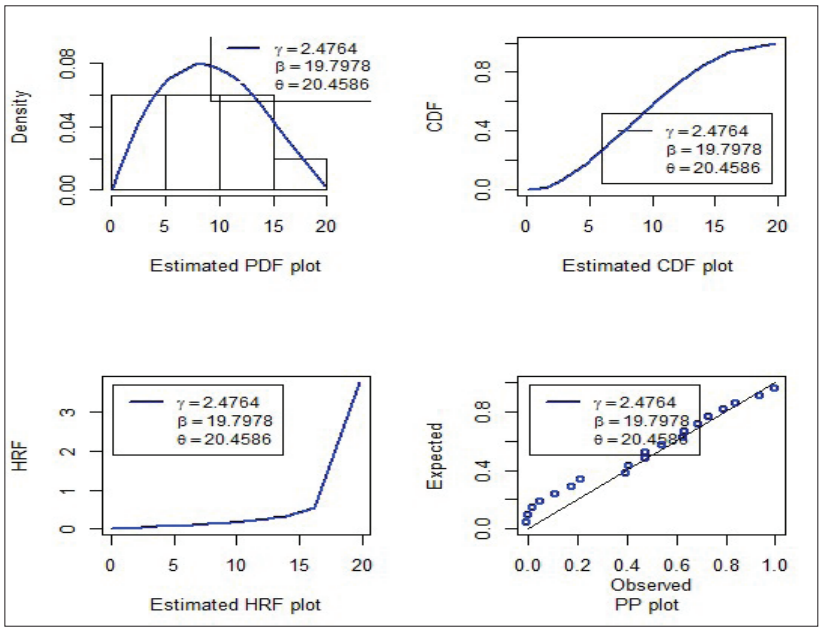

Figure 7: Some plots of the real dataset.

To assess the nature and behavior of the data, we employed several visualizations, including Box plot, Q-Q plots, total time in test (TTT) plot, and Kernal density estimation (KDE) plots for the real dataset, as shown in Figure 6. Using the same MLEs obtained for the goodness-of-fit measures, in Figure 7, some important plots are given. Additionally, the estimated density plot and HRF plots for the real dataset are illustrated in Figure 8. Figure 9 compares the AIC, BIC, CAIC, and HQIC values for the real dataset. These plots collectively demonstrate the advantage of the suggested distribution for the real-life dataset.

From Figures 6-9, it is clear that the SBRPF distribution is more appropriate to use for this data and demonstrate its flexibility to fit all types of data sets.

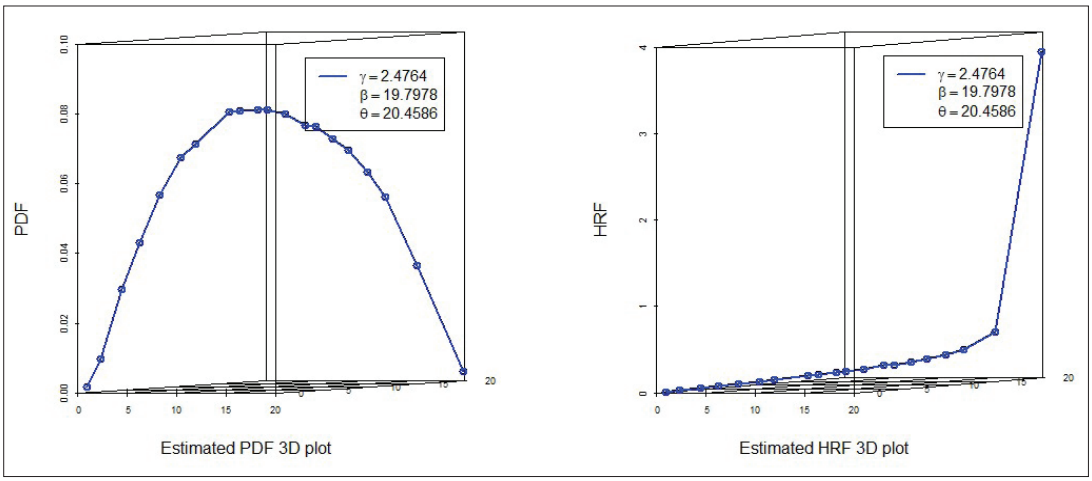

Figure 8: Estimated PDF (left panel) and estimated HRF (right panel).

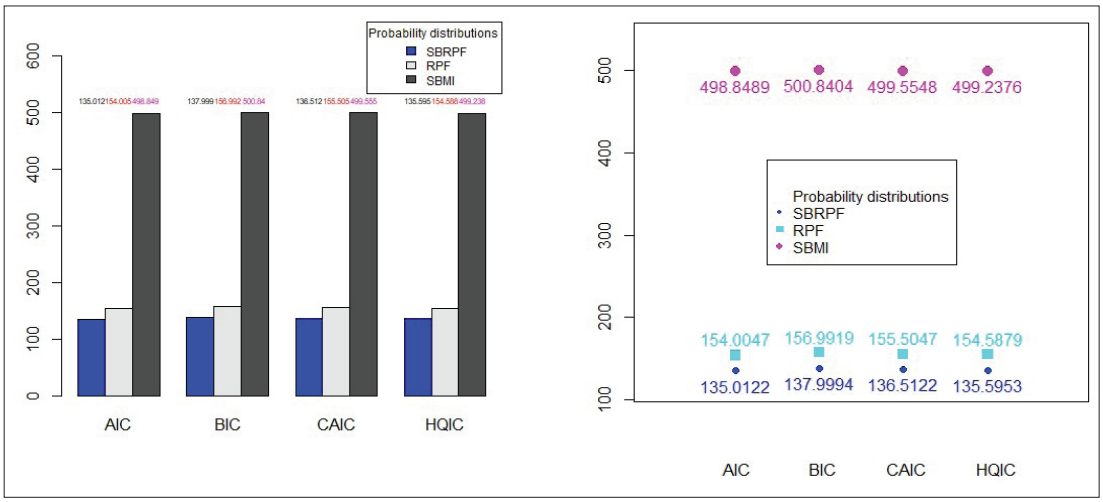

Figure 9: Evaluation of AIC, BIC, CAIC, HQIC for the real dataset.

Two proposed control monitoring

We introduce EWMA and EEWMA control charts, for MLEs of the SBRPF distribution. We utilized the R programming language to generate the results for these new control charts.

The EWMA control monitoring

The EWMA statistics, say $Z_{(t)}$, based on the MLEs of the SBRPF distribution is given by

$$A^*_{(t)} = \lambda^{**}\hat{\gamma}_{MLE(t)} , +(1-\lambda^{\&*})A^*_{(t-1)},$$

we observe $A^*_{(t)}$ as the EWMA statistic, and $A^*_{(t-1)}$ represents the previous value of the EWMA statistic. Also λ^{**} is smoothing constant and $\hat{\gamma}_{MLE(t)}$ is the maximum likelihood estimator of the shape parameter.

The EWMA control limits based on the MLEs of the SBRPF distribution are given by

$$UCL_{Z^*(t)} = \delta_0 + L\sqrt{Var(\hat{\gamma}_{MLE})\left[\frac{\lambda^{**}}{2-\lambda^{**}}\right][1-(1-\lambda^{**})^{2t}]}, \quad ...(15)$$

$$CL_{Z^*(t)} = \delta_0 \quad ...(16)$$

and

$$LCL_{Z^*(t)} = \delta_0 - L\sqrt{Var(\hat{\gamma}_{MLE})\left[\frac{\lambda^{**}}{2-\lambda^{**}}\right][1-(1-\lambda^{**})^{2t}]}. \quad ...(17)$$

The EEWMA control chart

The EEWMA statistics, say $E_{(t)}$, based on the MLE of the SBRPF distribution has the form $E_{(t)} = \varphi_1\hat{\gamma}_{MLE(t)} - \varphi_2\hat{\gamma}_{MLE(t-1)} + (1-\varphi_1+\varphi_2)\,E_{(t-1)}$, where $0 \le \varphi_1 \le 1,\ 0 \le \varphi_2 \le 1$,..

The EEWMA control limits based on the MLE of the SBRPF distribution are defined by

$$UCL_{E(t)} = \delta_0 + L\sqrt{Var(\hat{\gamma}_{MLE})\left[(\varphi_1{}^2+\varphi_2{}^2)*\left(\frac{1-(1-\varphi_1+\varphi_2)^{2i}}{1-(1-\varphi_1+\varphi_2)^2}\right)-2(1-\varphi_1+\varphi_2)\varphi_1\varphi_2\left(\frac{1-(1-\varphi_1+\varphi_2)^{2i-2}}{1-(1-\varphi_1+\varphi_2)^2}\right)\right]}, \quad ...(18)$$

$$CL_{E(t)} = \delta_0 \quad ...(19)$$

and

$$LCL_{E(t)} = \delta_0 - L\sqrt{Var(\hat{\gamma}_{MLE})\left[(\varphi_1{}^2+\varphi_2{}^2)*\left(\frac{1-(1-\varphi_1+\varphi_2)^{2i}}{1-(1-\varphi_1+\varphi_2)^2}\right)-2(1-\varphi_1+\varphi_2)\varphi_1\varphi_2\left(\frac{1-(1-\varphi_1+\varphi_2)^{2i-2}}{1-(1-\varphi_1+\varphi_2)^2}\right)\right]}. \quad ...(20)$$

Performance evaluation of the control monitoring

We have evaluated the control monitoring charts as follows:

1. Generate random data from the SBRPF distribution.
2. Compute $\hat{\gamma}_{MLE}$, for the data generated in step 1.
3. Repeat the first two steps 2,000 times to calculate ($\hat{\gamma}_{MLE}$).
4. Set control limits for the EWMA monitoring using step 3.
5. Fix ARL_0 for both proposed control charts, and for various shift values, compute ARL_1. Repeat similar steps for the EEWMA monitoring of the MLE.

The numerical results are reported in Table 4 and illustrated in Figure 11. The findings indicate that the EEWMA control monitoring based on $\hat{\gamma}_{MLE(t)}$, outperforms the EWMA control chart, as it detects shifts more quickly compared to the EWMA control monitoring.

Table 4: Evaluation indices for EWMA and the EEWMA monitoring of the MLE with $ARL_0 = 289$.

$ARL_0 = 289$		
Shifts	$EWMA \rightarrow ARL\ (\hat{Y}_{MLE(t)})$	$EEWMA \rightarrow ARL\ (\hat{Y}_{MLE(t)})$
0	289	289
0.05	289	276
0.1	288	74
0.12	284	74
0.14	281	74
0.6	239	17
0.7	237	17
1	196	17
1.3	172	12
1.6	153	10
2	91	10
4	1	1

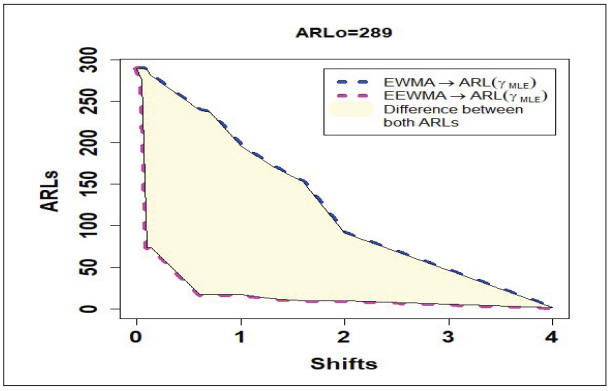

Figure 11: Comparison of EWMA and EEWMA control charts based on the MLE through ARLs with $ARL_0 = 289$.

Simulation results

A simulation study was conducted for the EWMA and EEWMA control charts based on the MLE of the SBRPF distribution. Initially, random observations were generated from the SBRPF distribution with parameters $(\gamma, \beta, \theta) = (1,2.1,5)$ to compute $\hat{Y}_{MLE}$. This process was repeated for 40 samples to obtain the EWMA statistics $Z_{(t)}$ and the control limits for the EWMA control chart. The $Z_{(t)}$ values were plotted against the subgroups (samples) in Figure 12.

The same procedure was followed for the EEWMA monitoring charts. The results are summarized in Table 5 and illustrated in Figure 12.

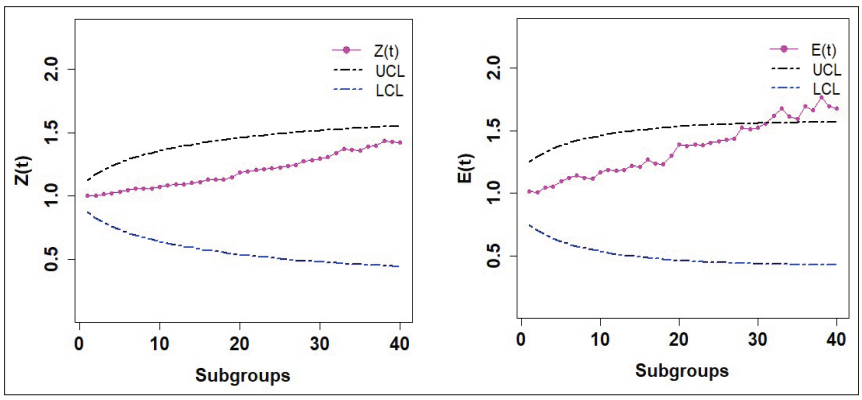

Figure 12: The EWMA and EEWMA monitoring of the MLE.

Table 5: Simulated results of the EWMA and EEWMA monitoring for the MLE.

EWMA $\lambda = 0.02$, L=10			EEWMA $\varphi_1 = 0.065$, $\varphi_1 = 0.02$, L = 6		
Z	UCL	LCL	E	UCL	LCL
1.004759	1.122616	0.877384	1.015465	1.250164	0.749836
1.004711	1.17168	0.82832	1.010166	1.29336	0.70664
1.016776	1.208186	0.791814	1.049179	1.327831	0.672169
1.022649	1.238034	0.761966	1.054982	1.356373	0.643627
1.037417	1.263536	0.736464	1.095768	1.380543	0.619457
1.050256	1.285894	0.714106	1.120398	1.401319	0.598681
1.061347	1.305832	0.694168	1.140704	1.419371	0.580629
1.060174	1.323827	0.676173	1.122451	1.435182	0.564818
1.059182	1.340215	0.659785	1.117574	1.449117	0.550883
1.075557	1.355243	0.644757	1.169138	1.46146	0.53854
1.087668	1.3691	0.6309	1.18824	1.472435	0.527565
1.090424	1.381935	0.618065	1.180801	1.482228	0.517772
1.094004	1.393869	0.606131	1.185671	1.490988	0.509012
1.106353	1.404999	0.595001	1.21817	1.498844	0.501156
1.109638	1.415408	0.584592	1.211713	1.505902	0.494098
1.130199	1.425164	0.574836	1.270725	1.512255	0.487745
1.128672	1.434328	0.565672	1.239288	1.51798	0.48202
1.127428	1.442951	0.557049	1.231763	1.523148	0.476852
1.149125	1.451077	0.548923	1.298802	1.527817	0.472183
1.185884	1.458746	0.541254	1.390271	1.532039	0.467961
1.196176	1.465992	0.534008	1.378498	1.535861	0.464139
1.206009	1.472847	0.527153	1.392166	1.539322	0.460678
1.209137	1.479338	0.520662	1.384317	1.542461	0.457539
1.217346	1.485491	0.514509	1.400047	1.545307	0.454693
1.227212	1.491327	0.508673	1.415848	1.54789	0.45211
1.236997	1.496868	0.503132	1.42949	1.550235	0.449765
1.244325	1.502131	0.497869	1.435054	1.552365	0.447635
1.27621	1.507135	0.492865	1.522916	1.554301	0.445699
1.284237	1.511895	0.488105	1.506657	1.55606	0.44394
1.294075	1.516424	0.483576	1.520755	1.55766	0.44234

While comparing EWMA and EEWMA, Figure 12 indicates that the process is out of control starting from observation 32, leading to the conclusion that corrective actions may be necessary. This detection is given by EEWMA, making it more powerful Control monitoring as compared to EWMA for SRPF distribution.

Real data application

Here, we extend the EWMA and EEWMA with real-life data of "Electronic Component Failure time," sourced from [39]. The resulting plots based on this data are shown in Figure 14.

Table 5: Simulated results of the EWMA and EEWMA monitoring for the MLE (continued).

EWMA $\lambda = 0.02$, L=10			EEWMA $\lambda_1 = 0.065$, $\lambda_2 = 0.02$, L=6		
Z	UCL	LCL	E	UCL	LCL
1.309651	1.520738	0.479262	1.551534	1.559115	0.440885
1.338554	1.524847	0.475153	1.619321	1.560439	0.439561
1.368199	1.528763	0.471237	1.674705	1.561644	0.438356
1.360935	1.532497	0.467503	1.608254	1.56274	0.43726
1.35676	1.536059	0.463941	1.590673	1.563738	0.436262
1.390283	1.539458	0.460542	1.693191	1.564647	0.435353
1.394637	1.542702	0.457298	1.660857	1.565474	0.434526
1.430629	1.545799	0.454201	1.761584	1.566228	0.433772
1.425408	1.548758	0.451242	1.694449	1.566915	0.433085
1.420938	1.551584	0.448416	1.672931	1.56754	0.43246

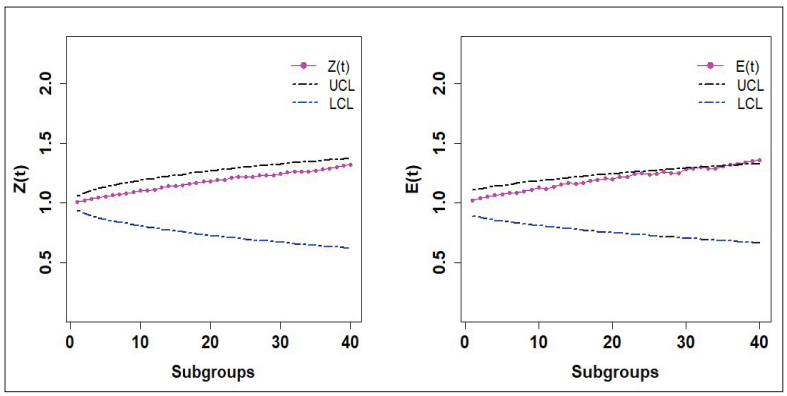

Figure 14: The EWMA and EEWMA monitoring of MLE for the real dataset.

In Figure 14, the EWMA and EEWMA monitoring of MLE are presented. In the right panel of Figure 14 that is the result of EEWMA, indicators show that the process is out of control from observation 36 onward. So once again EEWMA proved itself as best control monitoring to be used for SBRPF distribution.

CONCLUSION

In this research, we initially present the model identification for the proposed distribution. We investigate various properties of this distribution and discuss estimation methods, demonstrating the consistency of the mean squared error (MSE) for all estimators derived from both types of estimation methods. We also apply the proposed distribution to real data, providing a summary of the data, goodness-of-fit measures, and numerous plots. These results illustrate that our proposed distribution outperforms several existing distributions. Additionally, we implement EWMA and EEWMA control charts based on the maximum likelihood estimation (MLE) of the SBRPF distribution, highlighting its practical applications. From both Simulation studies and real life application, we observe that EEWMA is more effective control chart for detecting early change during a process for SBRPF distribution.

Funding

Princess Nourah bint Abdulrahman University Researchers Supporting Project number (PNURSP2026R735), Princess Nourah bint Abdulrahman University, Riyadh,Saudi Arabia.

REFERENCES

Ahmad, M., Jabeen, R., Zaka, A., Hamdi, W. A. and Alnssyan, B. (2024) A unified generalized family of distributions: Properties, inference, and real-life applications. *AIP Advances 14*, 015043, https://doi.org/10.1063/5.0187188.

Abbasi, W. M., Ahmad, S., Perveen, S. and Rehman, T. (2017). Preliminary phytochemical analysis and invivo evaluation of antipyretic effects of hydro-methanolic extract of Cleome scaposa leaves. *Journal of Traditional and Complementry Medicine, 8*(1) (2017) 147-149. https://doi.org/10.1016/j.jtcme.2017.05.004.

Afify, A. Z., and Mohamed, O. A. (2020). A new three-parameter exponential distribution with variable shapes for the hazard rate: estimation and applications. *mathematics, 8*(1), 135. https://doi.org/10.3390/math8010135.

Brereton, C. F., and Jagals, P. (2021). applications of systems science to understand and manage multiple influences within children's environmental health in least developed countries: a causal loop diagram approach. *International Journal of Environmental Research and Public Health, 18*(6), 3010. https://doi.org/10.3390/ijerph18063010.

Cohen, A. C. (1973). The reflected Weibull distribution. *Technometrics, 15*(4), 867-873. https://doi.org/10.2307/1267396.

Crowder, S. V. and Hamilton, M. D. (2018). An EWMA for monitoring a process Standard Deviation. *Journal of Quality Technology, 24*(1) (2018) 12-21. https://doi.org/10.1080/00224065.1992.11979369.

Dar, A. A., Ahmed, A. and Reshi, J. A. (2017). Transmuted weighted exponential distribution and its application. *Journal of Statistics Applications and Probability, 6*(1), 219-232. https://doi.org/10.18576/jsap/060117.

Dallas, A. C. (1976). Characterizing the pareto and power distributions. *Annals of Institute of Statistical Mathematics 28*, 491–497. https://doi.org/10.1007/BF02504764.

Dennis, B. and Patil, G. (1984). The gamma distribution and weighted multimodal gamma distributions as models of population abundance. *Mathematical Biosciences, 68*(2), 187-212. https://doi.org/10.1016/0025-5564(84)90031-2.

Fisher, R. A. (1934). The effect of methods of ascertainment upon the estimation of frequencies. *Annals of Human Genetics. 6*(1), 13-25. https://doi.org/10.1111/j.1469-1809.1934.tb02105.x.

Grosenbaugh, L. R. (1958). Point-sampling and line-sampling probability theory, geometric implications, Synthesis. USDA Forest Service, Southern Forest Experiment Station, Occasional Paper 160.

Gove, J. H. and Patil, G.P. (1998) Modeling the basal area-size distribution of forest stands: acompatible approach. *Forest Science 44*(2), 285-297.

Huwang, L., Wu, C. H. and Lee, Y. R. (2021). EWMA and adaptive EWMA variable sampling intervals charts for simultaneous monitoring of Weibull parameters. *Quality Technology and Quantitative Management. 18*(5), 552-575. https://doi.org/10.1080/16843703.2021.1918439.

Jabeen, R., Ahmad, M., Zaka, A., Mansour, M. M., Aljadani, A. and Elrazik, E. M. (2024). A new statistical approach based on the access of electricity application with some modified control charts. *Journal of Mathematics*, 2024, Article ID 6584791. https://doi.org/10.1155/2024/6584791.

Jabeen R., Akhtar, A. and Zaka, A. (2023). Modified calibrated control charts for monitoring the population mean under stratified sampling. *Quality and Reliability Engineering International 2023*; *39*, 143–163. https://doi.org/10.1002/qre.3225.

Jabeen, R., Zaka, A. and Khan K. I. (2022). Classical estimator based modified control charts for phase-II monitoring in real life. *Quality and Reliability Engineering International 2022; 38*, 2862–2880. https://doi.org/10.1002/qre.3112.

Kao, J. H. (1958). Computer methods for estimating Weibull parameters in reliability studies. *IRE Transactions on Reliability and Quality Control, 13*, 15–22. https://doi.org/10.1109/IRE-PGRQC.1958.5007164.

Kao, J. H. (1959). A graphical estimation of mixed Weibull parameters in life testing electron tube. *Technometrics, 1* (1959) 389-407. https://www.jstor.org/stable/1266719.

Kranich, G. D. (2016). Inconsistent conceptions of acceleration contributing to formative assessment limitations, Electronic Theses and Dissertations. 2438. https://digitalcommons.library.umaine.edu/etd/2438.

Lappi,J and Bailey,R.L. (1987). Estimation of the diameter increment function or other tree relations using angle-count samples. *Forest Science. 33*(3) (1987) 725-739. https://doi.org/10.1093/forestscience/33.3.725

Mahfoud,M and G.P. Patil,G.P.(1982). On Weighted Distributions, Statistics and Probability, New York, (1982), 479-492.

Meniconi, M., Barry, D. M. (1996). The power function distribution: A useful and simple distribution to assess electrical component reliability. *Microelectronic Reliability, 36*(9), 1207–1212. https://doi.org/10.1016/0026-2714(95)00053-4

Montgomery D.C. (2012). Introduction to Statistical Quality Control, 7th edition. John Wiley and Sons, New York, USA.

Murthy,D.N., Xie,M and Jiang, R. (2004). Weibull Models. Wiley. ISBN: 978-0-471-47327-5.

Mutairi, A. A., Iqbal, M. Z. Arshad, B. Al-Mofleh, A. H. and Afify, A. Z. (2021). A new extended model with bathtub-shaped failure rate: properties, inference, simulation, and applications. *Mathematics. 9*(17) (2021). https://doi.org/10.3390/math9172024.

Naveed, M., Azam, M., Khan, N. and Aslam, M. (2018). Design of a control chart using extended EWMA statistic. *Technologies. 6*(4) (2018) 108. https://doi.org/10.3390/technologies6040108.

Ozsan, G., Testikb, M. C. and Weiß, H. (2010) Properties of the exponential EWMA chart with parameter estimation. *Quality and Reliability Engineering International, 26* (2010) 555-569. https://doi.org/10.1002/qre.1079.

Pascual,F. (2010). EWMA charts for the Weibull shape parameter. *Journal of Quality Technology, 42*(4) (2010)

400-416. https://doi.or\g/10.1080/00224065.2010.11917836.

Patil,G.P and Ord,J.K. (1976). On Size-Biased Sampling and Related Form-Invariant Weighted Distributions. *Industrial Journal of Statistics. 38*(1) (1976) 48- 61.

Patil,G.P.(1981). Studies in statistical ecology involving weighted distributions. In Proceedings of the Indian statistical Institute, Calcutta. (1981) 478-503.

Rao, C. R. (1965). On discrete distributions arising out of methods of ascertainment. In classical and contagious discrete distributions. Pergamon Press and Statistical Publishing Society, Calcutta, 320-332. https://www.jstor.org/stable/25049375

Roberts, S. W. (2000). Control chart tests based on geometric moving averages. *Technometrics, 42*(1), 97–101. https://doi.org/10.1080/00401706.2000.10485986

Siddiqui, S. A., Dwivedi, S., Dwivedi, P. and Siddiqui, I. (2016). Development of Size-Biased Mukherjee-Islam Distribution. *International Journal of Pure and Applied Mathematics, 107*(2) (2016) 505-515. https://doi.org/10.12732/ijpam.v107i2.18.

Taillie, C., Patil, G.P. and Hennemuth, R. (1995) Modeling and analysis of recruitment distributions. *Ecological and Environmental Statistics 2*(4), 315-329.

Warahena-Liyanage, G. B., Oluyede, T. Moakofi, T and W. Sengweni, W. (2023). The new exponentiated half logistic-Harris-G family of distributions with actuarial measures and applications. *Stats. 6,* (2023) 773–801, https://doi.org/10.3390/stats6030050.

Yu,D., Jin,L.L., Li,J., Qin,X., Z. Zhu,Z.and Zhang,J.(2023) Monitoring the Weibull scale parameter based on type I censored data using a modified EWMA control chart. *Axioms, 12*(5) (2023) 487.https://doi.org/10.3390/axioms12050487.

Zaka A., Akhter A.S. & Jabeen R. (2020). The new reflected power function distribution: theory, simulation and application. *AIMS Mathematics 5*(5): 5031–5054. https://doi.org/10.3934/math.2020323.

Zaka, A., Jabeen, R and Khan, K.I. (2021). Control charts for the shape parameter of skewed distribution. *Intelligent Automation & Soft Computing, 30*(3), 1007–1018. https://doi.org/10.32604/iasc.2021.016491.

Zeineldin ,R.A., Chesneau ,C., Jamal ,F and Elgarhy,M,(2019). Different estimation methods for type i half-logistic topp–leone distribution. *Mathematics, 7*(10) (2019) 985, https://doi.org/10.3390/math710098.